

## **Fibrous \*PCL melt electrospun scaffolds for wound healing applications**

**Matteo Gazzarri<sup>^</sup>, Cristina Bartoli<sup>^</sup>, Carlos Mota, Dario Puppi, Dinuccio Dinucci, Silvia Volpi, Federica Chiellini\***

Laboratory of Bioactive Polymeric Materials for Biomedical and Environmental Applications (BIOLab), Department of Chemistry and Industrial Chemistry, University of Pisa, via Vecchia Livornese 1291, 56010 San Piero a Grado (Pi), Italy

<sup>^</sup> These authors contributed equally to the work.

\*Corresponding author: Dr. Federica Chiellini, Department of Chemistry & Industrial Chemistry, University of Pisa (Pisa, Italy); e-mail: federica@dcci.unipi.it; Tel: +39-050-2210305; Fax: +39-050-2210332

**Keywords:** Melt electrospinning, Star poly(e-caprolactone), Wound dressing, Co-culture, Fibroblasts, Keratinocytes.

### **ABSTRACT**

Polymeric fibrous scaffolds based on the biocompatible and biodegradable three arm branched star poly(e-caprolactone) (\*PCL), ( $M_w = 189000$  g/mol) were prepared by melt electrospinning (Melt-ES) technique. The possibility of processing polymers without the use of organic solvents is one of the main advantages over solution electrospinning. Scaffolds were submitted to biological investigations to assess their ability of supporting skin tissue regeneration. For this purpose, mouse embryo fibroblast (balb/3T3 clone A31) and human keratinocyte (HaCaT) cell lines were selected as models and seeded onto the polymeric supports both as single and co-culture. Cell viability, proliferation and collagen production were assessed by WST-1 assay and Direct Red 80 dye, respectively. Cell morphology and

colonization of the supports were evaluated by scanning electron microscopy (SEM) and confocal laser scanning microscopy (CLSM). Results highlighted that the developed \*PCL scaffolds were able to promote collagen production by fibroblasts. In co-culture studies scaffolds supported adhesion, proliferation, and spatial organization of both cell lines. In virtue of the observed results, the developed polymeric scaffolds appeared suitable as biodegradable and biocompatible three-dimensional (3D) supports for skin tissue regeneration in wound healing dressing.

## **INTRODUCTION**

Skin is the largest organ of the body in vertebrates and plays a crucial role in many physiological functions <sup>1</sup>. The skin forms a self-renewing and self-repairing interface between the body and the environment <sup>2</sup>. It protects against toxins and microorganism in the environment and serves to prevent dehydration maintaining fluid homeostasis. Skin gets involved with sensory stimuli detection, immune surveillance and other critical functions. Loss of skin integrity because of injury or illness may result acutely in substantial physiologic imbalance and ultimately in significant disability or even death <sup>3</sup>.

Skin is composed of epidermis and dermis. The first mainly consists of layers of keratinocytes separated from the dermis by the basement membrane. The second one underlies the epidermis and is composed of the predominating extracellular matrix (ECM) proteins, such as collagen, elastin and glycosaminoglycans and the cellular constituents of mainly fibroblasts <sup>1</sup>.

Wounds that extend partially through the dermis are capable of regeneration, but unfortunately the body cannot heal deep dermal

injuries adequately <sup>2</sup>. Dermal wounds caused by mechanical trauma, surgical procedures, burns, chemicals or diseases are conventionally treated using autografts, allografts and xenografts. Although autografts are gold standards, their use has been constrained due to their limited availability in the case of severely burnt patients and also donor site morbidity. On the other hand, allografts and xenografts are available in plenty but pose the risk of disease transmission and immune response <sup>4</sup>. Over the past three decades, extraordinary advances and improved understanding in cell/molecular biology have led to achievements in skin tissue regeneration for wound healing <sup>5 1</sup>. Tissue engineered skin, based on the concept of a cell-matrix construct, represents a significant advancement in the field of wound healing and has emerged as promising alternative to the grafting techniques due to its inherent advantages. Tissue engineering employs tissue specific cells in a nano and microfibrous structure that mimics the three-dimensional (3D) organization of the native tissue thus providing the functionality of any diseased or damaged organ <sup>4</sup>. In recent years, there has been an increasing interest in electrospinning (ES) technology for the fabrication of the scaffolds for tissue engineering <sup>6-11</sup>. This technique produces non-woven membranes with individual fiber diameters ranging from a few nanometers to hundreds of nanometers, which mimics the structure and the function of natural ECM. In this respect, electrospinning can be utilized for manufacturing wound dressing materials, which promote faster restoration and increase biocompatibility. The fibers can be made to form a porous structure that is ideal for drugs, genes, growth factors, in order to influence cell functions, as well as cell delivery <sup>2, 12</sup>. Moreover, even greater control of cellular

response can be achieved by attaching bioactive peptides to the fiber surfaces <sup>13</sup>.

Electrospinning can be performed with various polymers both in solution and in melt (Melt-ES) <sup>14</sup>. Melt-ES allows new approaches to various applications offering several advantages over solution electrospinning such as the overcoming of technical restrictions due to solvent accumulation and toxicity <sup>15, 16</sup>. Nevertheless, Melt-ES technique is not able to attain fibers in nanometer range because of high viscosity of the melt polymeric jet. However an increase in fiber diameter facilitates increased pore size and interconnectivity, which has benefits for cells penetration into the scaffold structure <sup>17</sup>.

Electrospun scaffolds can be fabricated using both synthetic and natural polymers, as well as composite or blended materials. Among synthetic polymers, star polymers are constituted of a number of linear polymeric chains attached to a relatively small central moiety <sup>18</sup>. Due to their small size, spherical structure and limited interaction between molecules, star polymers have unique properties particularly compared with linear polymers with equivalent molecular weight, such as reduced viscosity and better control over chain end concentration, which is exploitable for tailored functionalization and controlled degradation <sup>18, 19</sup>. A number of studies have been recently devoted to the development of biodegradable star-shaped polymers with arms made of aliphatic polyesters, such as poly( $\epsilon$ -caprolactone) (PCL) <sup>20</sup> and poly(L-lactide) <sup>21</sup>, bound by a central core. Xie *et al.* <sup>20</sup> showed that the crystallinity and biodegradation rate of star-shaped PCL<sub>s</sub> with two to five arms could be varied by changing the arms length. A three-arm branched star poly( $\epsilon$ -caprolactone) (\*PCL) <sup>22, 23</sup> has



been investigated in the last years for the development of microfibrous scaffolds by either solution electrospinning<sup>24</sup> or wet-spinning<sup>25-27</sup> showing good compatibility to preosteoblast cells. In addition, \*PCL microfibrous meshes have been recently developed by Melt-ES Writing technique and characterized as potential substitutes suitable for use as tissue engineering applications<sup>28</sup>. In particular, the microscale topography of the developed scaffolds similar to the natural ECM suggested their employment in wound dressing applications. Nevertheless, the cellular heterogeneity that exists in a healing tissue raises the question of how a cell type influences another. One of the most powerful tools to study cellular crosstalk is the co-culture system, to better understand the mechanisms of tissue regeneration<sup>29</sup>. Co-culture of mouse fibroblasts and human keratinocytes were used in order to verify the suitability of these constructs to provide structural integrity and mechanical strength to skin tissues in the wound healing course.

## **MATERIALS AND METHODS**

### **Materials**

Three-arm star branched poly( $\epsilon$ -caprolactone) \*PCL (Mw = 189000 g/mol) was supplied by **Professor Ramani Narayan of Michigan Biotechnology Institute (Lansing, MI, USA)**.

### **Preparation of melt electrospun scaffolds**

Three-dimensional \*PCL scaffolds were prepared by means of a melt extrusion-based additive manufacturing (AM) system enabling layer-by-layer fabrication of 3D structures composed by melt-electrospun polymeric fibres, as previously described<sup>28</sup>. **Briefly, the polymer was loaded into a reservoir and kept at 160°C for 1 h**

to allow complete melting. Afterwards a nitrogen gas pressure (5 bar) was applied to force the polymer melt to a screw extruder that control the polymer flow through an electrically grounded nozzle (inner diameter 340  $\mu\text{m}$ , length 5mm). A 10×10  $\text{cm}^2$  copper plate was positioned on top of the construction platform and connected to a high voltage power supply (SL70P60/230, Spellman High Voltage Electronic Corporation, UK) to generate an electric field. The deposition pattern employed to fabricate scaffolds layer-by-layer was calculated using a Matlab (MathWorks Inc., MA) algorithm. A square cuboid model characterized by a base measuring 30×30  $\text{mm}^2$ , a distance between the axis of the parallel deposition lines of 2 mm, and five overlapped layers (0–90° lay-down pattern) was designed. The nozzle X–Y translational velocity was 500  $\text{mm min}^{-1}$  and the distance between the nozzle tip and the collector was 10 cm. By employing an auxiliary IR lamp (150 W, Philips, Netherland) the ambient temperature and humidity inside the spinning chamber was kept at 35±2 °C and 22%±4%, respectively.

### **Morphological analysis**

The morphology of the produced meshes was investigated using a scanning electron microscope (SEM, JEOL LSM 5600 LV, Japan) at different magnification (50X-2000X).

## **Cell culture**

Mouse embryo fibroblasts balb/3T3 clone A31 cell line (CCL-163) was purchased from American Type Culture Collection (ATCC) and human keratinocytes HaCaT cell line was obtained from CLS (Cell Lines Service, Eppelheim, Germany). Fibroblasts were propagated using Dulbecco's Modified Eagle Medium (DMEM) (Sigma, Milan, Italy), supplemented with 4 mM of L-glutamine (Lonza, Milan, Italy), 1 % of penicillin:streptomycin solution (10,000 U/ml:10 mg/ml) (Lonza, Milan, Italy), 10% of calf serum (Sigma, Milan, Italy) and antimycotic (DMEM\_F). Keratinocytes were maintained in DMEM (Sigma, Milan, Italy), supplemented with 2 mM of L-glutamine (Lonza, Milan, Italy), 1 % of penicillin:streptomycin solution (10,000 U/ml:10 mg/ml) (Lonza, Milan, Italy), 10% of fetal bovine serum (Lonza, Milan, Italy) and antimycotic (DMEM\_K). Cells were grown at 37° C in a humidified CO<sub>2</sub> (5%) atmosphere. Fibrous \*PCL scaffolds with a thickness of 1,2 mm, were cut into pieces of about 1 cm<sup>2</sup> and sterilized by exposing to UV light for 30 min on each side<sup>4, 12, 30</sup>. Subsequently, scaffolds were soaked in 70% ethanol/water solution for 24 h, washed extensively with Dulbecco's Phosphate Buffer Saline (DPBS) added with penicillin/streptomycin solution (1%) pH 7.4 and conditioned overnight in DMEM\_F<sup>31</sup>. For studies of cell adhesion, proliferation, collagen production and morphology balb/3T3 clone A31 and HaCaT cell lines were seeded onto \*PCL constructs at a density of 2x10<sup>4</sup>/cm<sup>2</sup> and 1x10<sup>6</sup>/cm<sup>2</sup> respectively, in 1 ml of complete medium according to the literature<sup>32</sup>.

### **Cell proliferation assay**

The evaluation of cell proliferation was carried out on 3T3 and HaCaT cell lines cultured in single and co-culture onto \*PCL scaffolds. The proliferation rate was measured at day 3, 7, 10, 14 and 16 after seeding, using WST-1 cell proliferation reagent (Roche Diagnostic, Monza, Italy) as previously described <sup>33</sup>. To create a co-culture of 3T3-HaCaT with the ability to form a stratified epidermis in culture, fibroblasts were seeded on \*PCL scaffolds. On day 7 keratinocytes were directly seeded onto the fibroblast seeded-scaffolds and cells were allowed to proliferate until day 16 in DMEM\_K medium. Percentages of cell proliferation were normalized on the basis of single and co-culture cultured on tissue culture polystyrene (TCPS) plates.

### **Collagen production**

Mouse embryo fibroblasts balb/3T3 clone A31 were seeded on fibrous \*PCL scaffolds. Assessment of collagen production was carried out at days 3, 7 and 14. Scaffolds were washed twice with DPBS and then incubated with Direct Red 80 dye (Sigma, Milan, Italy) dissolved in picric acid (0.1%), for 1 h at room temperature. After the incubation time the dye was removed and samples were washed three times with HCl 10 mM to remove dye excess. The elution of the bound stain was performed with NaOH 0.1 N for 30 min at 37° C. Supernatants were aliquoted into 96 well plates and the absorbance was read at 540 nm <sup>34</sup>. Comparison of collagen production by cells grown in two-dimensions (2D) on TCPS under the same culture conditions was performed. Fibrous scaffolds and TCPS with no cells were treated following the same protocol and considered as blank. The photometric quantification of the collagen

was obtained by mean of a calibration curve prepared with collagen type I, derived from calf's skin (Sigma, Milan, Italy). Briefly, known concentrations of collagen in acetic acid (0.1 M) were filmed and dried on glass slides by solvent casting technique, in order to obtain a thin film. Films were then fixed and treated as the samples <sup>35</sup>.

### **Scanning electron microscopy**

Morphological analysis of balb/3T3 clone A31 cell line cultured in single and co-culture with HaCaT cell line on fibrous \*PCL scaffolds was carried out by scanning electron microscopy (SEM) at day 14 after seeding. After culture medium removal, each cell-cultured scaffolds was rinsed twice with DPBS, and the cells were fixed with 2% glutaraldehyde solution (Sigma, Milan, Italy) in phosphate buffer saline (PBS 1X). After 1 h of incubation, scaffolds were rinsed again with PBS 1X and treated with sodium cacodylate (0.1 M) pH 7.4 for approximately 1 minute. After cell fixation, specimens were dehydrated in ethanol solution of varying concentration (i.e. 10, 30, 50, 70, 90, and 100%, respectively) for 15 min at each concentration. Samples were dried in tetramethylsilane to remove any water traces. The fixed scaffolds were mounted on a SEM stub, coated with gold at 15 mA for 20 min, and observed by SEM at different magnifications (100X-2000X).

### **Confocal laser scanning microscopy**

Morphology and 3D culture organization of 3T3 cultured on \*PCL scaffolds were investigated by means of confocal laser scanning microscopy (CLSM) at days 3, 7 and 14 after seeding. Samples

were fixed with 3.8% paraformaldehyde for 30 min in PBS 1X, permeabilized with a PBS 1X/Triton X-100 solution (0.2%) for 10 min and incubated with a solution of 4'-6-diamidino-2-phenylindole (DAPI) (Invitrogen, Milan, Italy) and phalloidin-AlexaFluor488 (Invitrogen, Milan, Italy) in PBS for 45 min at room temperature in the dark. For characterization of keratinocytes, indirect immunofluorescence assay was carried out on cell co-culture at day 16 after seeding. Samples were washed three times with DPBS and fixed with 3.8% paraformaldehyde for 10 min. Samples were washed with PBS 1X, permeabilized with triton X-100 and incubated with BSA (1% w/v in PBS 1X) for 40 min. After further washing steps, samples were incubated for 60 min with the primary antibody anti-human cytokeratin clones AE1/AE3 (1:50 in PBS 1X) (Dako, Milan, Italy) and washed three times with PBS 1X. Subsequently, samples were incubated for other 60 min with the secondary antibody anti-mouse IgG-FITC conjugated (1:80 in PBS 1X) (Dako, Milan, Italy). Samples were then incubated with DAPI (2 ml/ml of PBS 1X) for 40 min. A Nikon Eclipse TE2000 inverted microscope equipped with an EZ-C1 confocal laser and Differential Interference Contrast (DIC) apparatus was used to analyze the samples at different magnification (10-20-60 and 100X). A 405 nm laser diode (405 nm emission) and an Argon Ion Laser (488 nm emission) were used to excite respectively DAPI and FITC fluorophores. Images were captured with Nikon EZ-C1 software with identical instrumental settings for each sample. Images were further processed with the GIMP (GNU Free Software Foundation) image manipulation software and merged with Nikon ACT-2U software.

## Statistical analysis

The *in vitro* biological tests were performed on triplicates, and the data are represented as mean  $\pm$  standard deviation. Statistical differences were analyzed using one-way analysis of variance (ANOVA)<sup>36</sup>, and a *p* value  $< 0.05$  was considered significant.

## RESULTS AND DISCUSSION

### Scaffolds properties

3D \*PCL melt-electrospun scaffolds were produced with a layer-by-layer approach by means of a melt extrusion-based AM system<sup>28</sup>. By applying the optimized processing parameters (i.e. processing temperature of 160°C, applied voltage of 25 kV and extrusion flow rate of  $3.7 \pm 0.08 \text{ ml}\cdot\text{h}^{-1}$ ), 3D meshes with a controlled external geometry and composed of five microfibrous layers were obtained (figure 1(a)). The electrospun non-woven fibrous structure (figure 1(b)) was characterized by a fibre diameter of  $40 \pm 5 \text{ }\mu\text{m}$  and a fully interconnected network of pores with size in the range of tens to hundreds of micrometres<sup>28</sup>.

The obtained layered structure appeared well suited as scaffold for the engineering of bidimensional tissues, such as skin, providing a cohesive microarchitecture with good integrity and a 3D microenvironment ideal for cell-cell interaction.

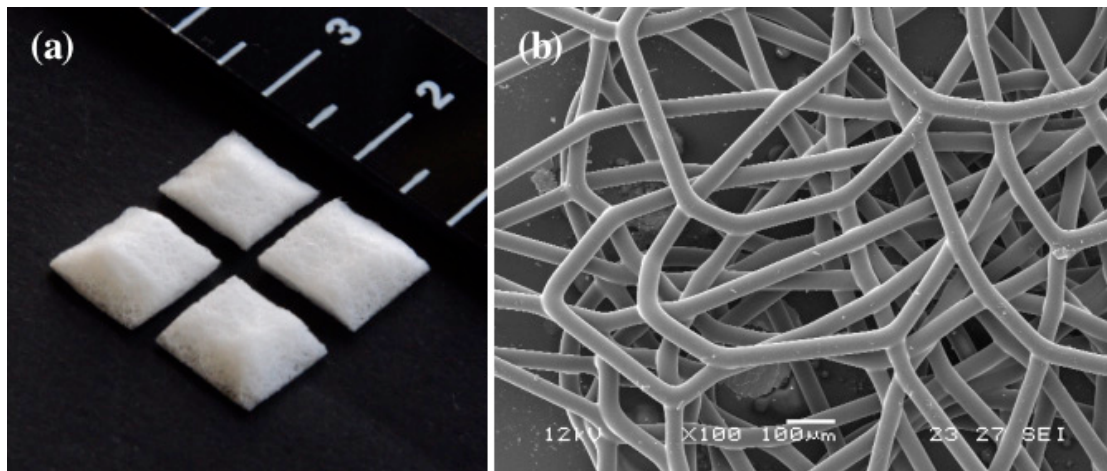


**Figure 1.** 3D \*PCL scaffolds by meltES: photograph (a) and representative SEM micrograph (b).

### Cell viability and proliferation

Balb/3T3 cells seeded on the prepared scaffolds showed increasing values of cell proliferation during the culturing period, as reported in figure 2.

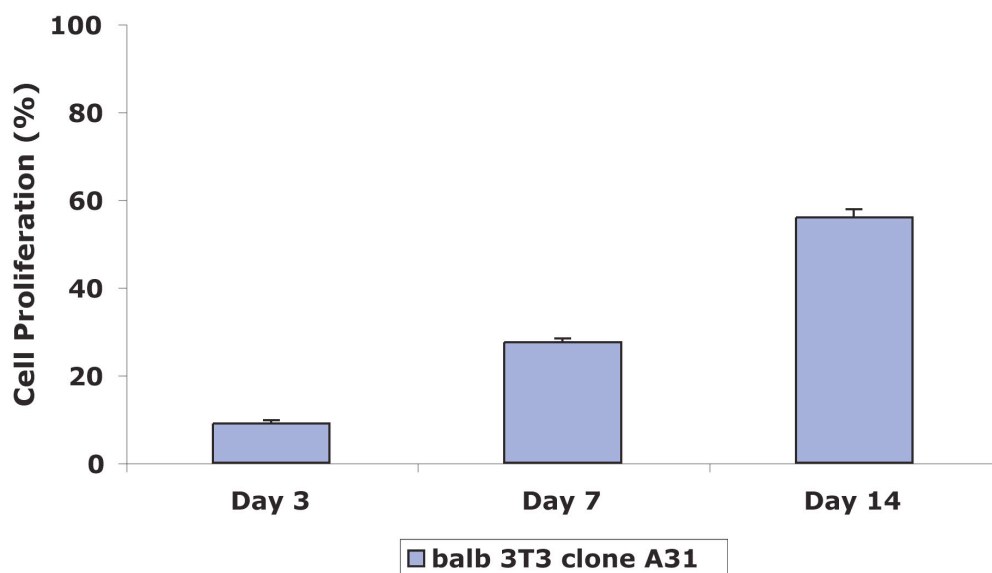


**Figure 2.** Cell proliferation of balb/3T3 clone A31 cultured on \*PCL based scaffolds compared with TCPS.

The spontaneously immortalized keratinocytes cell line HaCaT has been demonstrated to exhibit a high differentiation potential under



*in vivo* and *in vitro* conditions and thus has been extensively utilized as a substitute for normal human keratinocytes <sup>37</sup>. Consequently, HaCaT cells were selected for this study and seeded onto \*PCL scaffolds monitoring cell viability for 1 week. Results confirmed an absence of cell viability due to the fact that cells were not able to adhere and proliferate (data not shown). This behavior could be due to the lack of an adequate connectival substrate <sup>32</sup> associated to the poor hydrophilicity of \*PCL that could have negatively influenced the cell adhesion process <sup>38</sup>. To overcome this drawback, 3D heterologous organotypic co-cultures of mouse embryo fibroblasts and human keratinocytes were chosen. In organotypic co-cultures HaCaT cells form well-organized and differentiated epithelia in the presence of human or mouse embryonic fibroblasts <sup>32</sup> irrespective of the species and tissue origin of fibroblasts <sup>39 40</sup>. This is probably due to the homology of growth factors of both species, as also observed in 2D feeder-layer cultures <sup>41</sup>. Fibroblasts were then seeded on \*PCL based scaffolds and cultured for 7 days. Before HaCaT seeding, the presence of fibroblast monolayer on the constructs was confirmed from cell viability data (figure 2) and morphological CLSM analysis (§ 3.5 section). **Good values of cell proliferation, comparable to the ones of single culture, were obtained for the co-culture of 3T3 and HaCaT (figure 3).** Although it was not possible to distinguish the contribution of the single cell lines to the proliferation values of co-culture, results **confirmed** as a whole appreciable metabolic activity of the seeded cells. **Increasing values of cell proliferation of 3T3 single culture were observed at day 7,** with a weak decrease at days 10 and 14, probably due to the different type of culture medium, used for the co-culture (figure

3) as observed also in control samples on TCPS. Overall, preliminary biological evaluations suggested the suitability of the selected fibrous scaffolds to sustain the adhesion and the proliferation of the co-culture of balb/3T3 and HaCaT, with a promising role as biomimetic three-dimensional extracellular matrix, providing structural support to cells and a milieu for cell migration <sup>42</sup>.

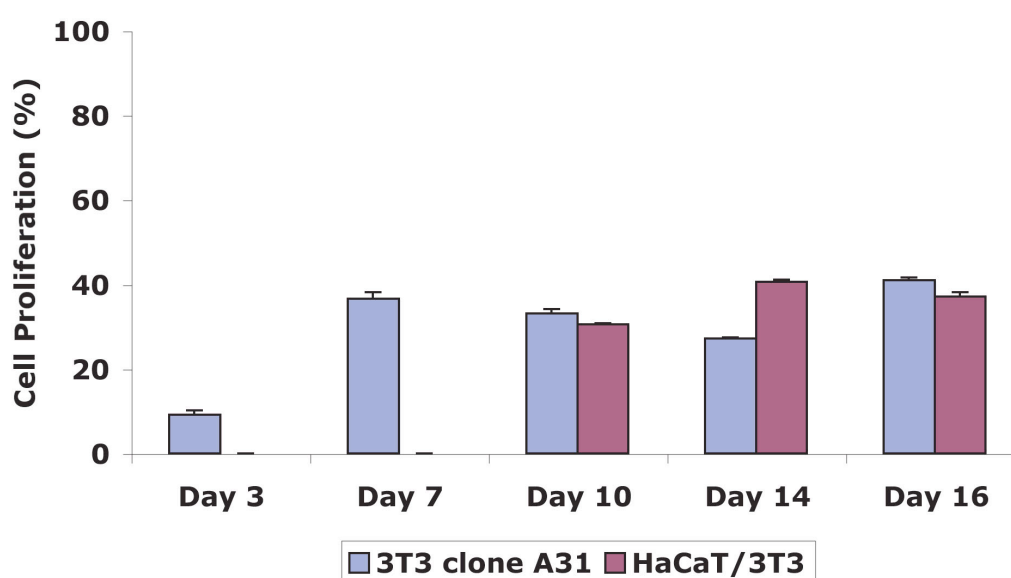


Figure 3. Cell proliferation of balb/3T3 clone A31 cultured on \*PCL based scaffolds in mono and co-culture with HaCaT, evaluated by WST-1 assay and compared with cells grown on TCPS.

### Collagen production

As reported by the literature <sup>43</sup>, to reproduce the normal physiology of epithelial tissue *in vitro* is necessary to use collagen supports or constructs populated with fibroblasts that are able to recreate the structural component of derma through the production of collagen and the secretion of growth factors that stimulate and regulate

keratinocytes proliferation <sup>44</sup>. Type I collagen, the predominant collagen form in human skin (80%), is produced mainly by fibroblasts and is important for cell adhesion and migration within connective tissues. Moreover, a significant enhancement in type I collagen expression was observed at the wound site (Huang 2012). For this purpose, collagen deposition from fibroblasts cultured on \*PCL meshes was estimated using the method of Direct Red 80 dye <sup>35, 45</sup> and compared with collagen produced from fibroblasts grown in 2D (TCPS). Values of collagen expressed as micrograms and obtained from 3T3 cultured on 3D \*PCL constructs and 2D TCPS were compared on the basis of the same values of cell proliferation expressed as absorbance of produced formazan measured at 450 nm (figure 4). Since the first three days of culture (Abs = 0.240) collagen produced in 3D condition **resulted to be significantly higher with respect to the values obtained in 2D culture** ( $p < 0.001$ ). Moreover, for longer culture times, 7 (Abs = 0.750) and 14 (Abs = 1.420) days, 3T3 cells cultured on fibrous \*PCL meshes showed an increased production of collagen 4-8 fold higher than cells cultured on TCPS ( $p < 0.001$ ). In the present studies type I collagen was selected for the calibration curve, because of his predominance in ECM. Since direct red 80 dye binds in a similar fashion to collagen I, II and III <sup>46</sup> the obtained collagen amount was slightly overestimated. Nevertheless, the observed trend between the production of collagen in 2D and 3D conditions was maintained. Thus, \*PCL scaffolds showed an excellent capability to induce 3T3 cells to synthesize and promote the deposition of collagen in continuous networks that form the structural ECM <sup>47</sup>. This result confirmed the suitability of the prepared scaffolds as ECM substitutes, providing an appropriate

environment for the engraftment of the keratinocytes, as supported from the previous data of cell proliferation (figure 4).

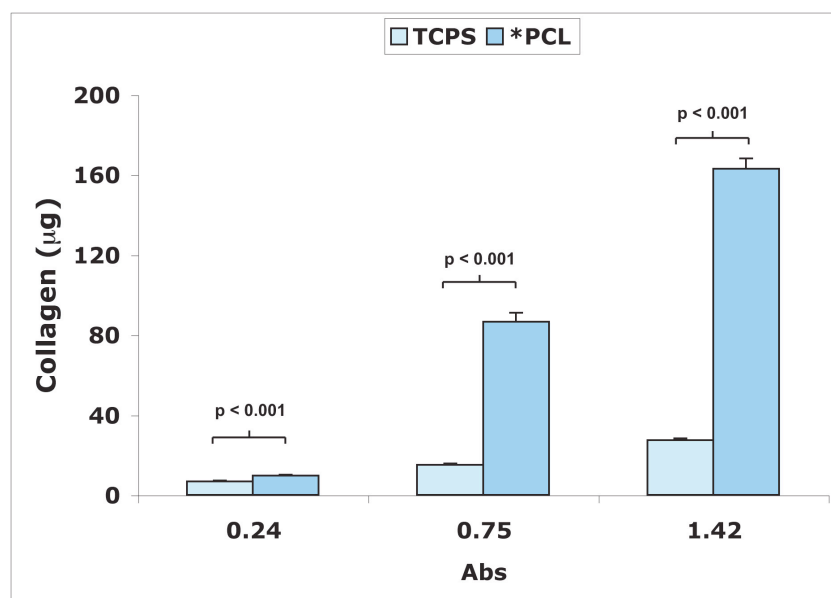


Figure 4. Collagen production obtained from balb/3T3 clone A31 cultured onto \*PCL meshes and on TCPS.

### Scanning electron microscopy

Scanning electron microscopy analysis allowed further characterization of the morphology and colonization of the balb/3T3 clone A31 cultured for 14 days on the fibrous \*PCL scaffolds. As shown in figure 5, 3T3 cells showed features indicative of cell activation, including numerous filopodia and fiber-like processes that allowed the anchorage of the cells to the substrate with the formation of a complex multicellular coverage<sup>48</sup>. 3T3 cells were able to colonize the scaffold surface with evident adhesion and spreading, confirming the previous data of cell proliferation and confocal laser scanning microscopy.

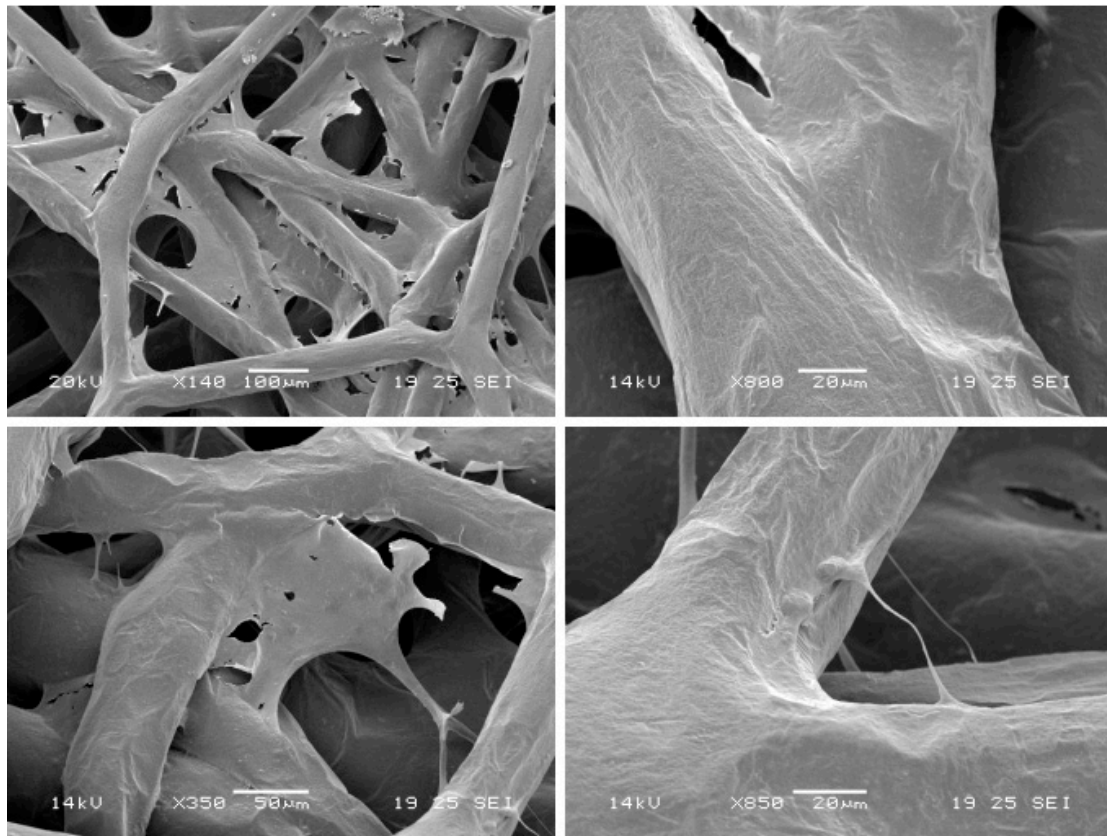


Figure 5. SEM images of balb/3T3 clone A31 grown on \*PCL scaffolds.

Further analysis allowed for emphasizing the morphology of the fibroblasts and keratinocytes grown in co-culture and the way of colonization of the fibrous \*PCL scaffolds, as well as to confirm the presence of both cell lines. As shown in figure 6, 3T3 cells were able to colonize the entire polymeric surface of the scaffold, adhering and diffusing in every direction and confirming quantitative data of cell proliferation. **The presence of a 3D cellular net and features indicative of cell activation were highlighted by SEM analysis**<sup>48</sup>. In particular, on the top of the scaffold, at the air-liquid interface, there was a clear prevalence of keratinocytes that formed a continuous cell layer with the presence of keratin scales, resembling a stratified and cornified epithelium. HaCaT colonization was noticed around and at the intersections of

polymeric fibers (figure 6(a-c)). Moreover, the presence of keratinocytes was observed also in the cross-section of the scaffold (figure 6(d-f)). Nevertheless, it was assumed that the multicellular coverage could be developed because of the extended underlying presence of fibroblasts that promote the adhesion and proliferation processes. In fact, an accurate observation of the bottom of the scaffold highlighted the prevalence of fibroblasts, detectable for the presence of numerous filopodia and fiber-like processes that allowed for the anchorage to the fibers (figure 6(g-i)). Tendency of the cells to colonize in a different way different areas of the scaffold could be due to intrinsic ability of the cells to auto-organize them self in a 3D structure because of biochemical signals as growth factor and cytokines <sup>49</sup>. Moreover, as reported by the literature <sup>50</sup>, the organization and the differentiation of keratinocytes cultured on 3D constructs is closely related to the stimuli derived from the different culture conditions, as the growth of the culture at the air-liquid interface <sup>49</sup>.

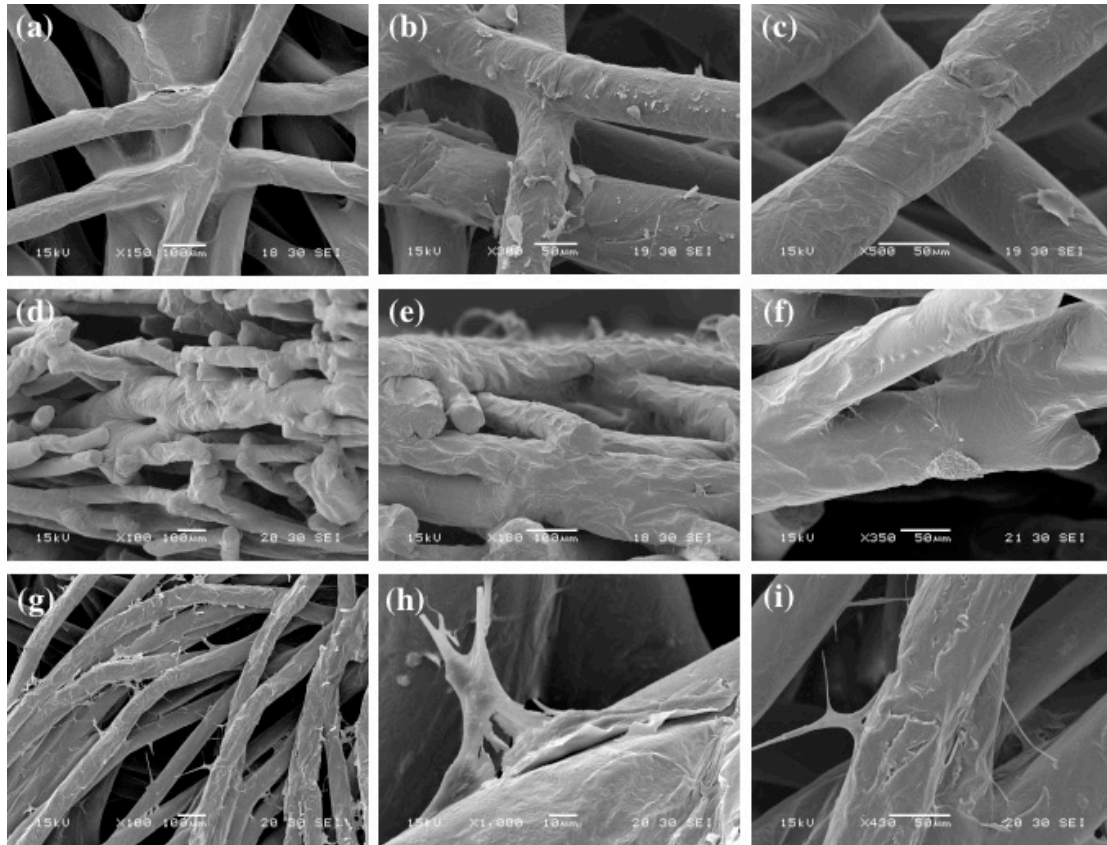


Figure 6. SEM images of co-cultures grown on the \*PCL scaffolds: top (air-liquid interface) (a-c), cross-section (d-f) and bottom (g-i).

### **Confocal laser scanning microscopy**

Cell morphology and cytoskeletal structure of 3T3 grown on the prepared \*PCL scaffolds were observed with a CLSM microscopy. The adherent cells were stained for F-actin with FITC-phalloidin and nucleus was stained with DAPI. Cells, observed with a 20X magnification, displayed a spread out, both spindle and stellate shapes <sup>12</sup> with dendritic (arm-like) extensions from the cell membrane anchoring the cells across the fibrous substrate (figure 7). Cell architecture showed consistent F-actin organization with early stages of cell adaptation to the material, <sup>51, 52</sup>, exhibiting great stress fibers stretched along the cytoplasm. At the third day of culture, a reduced presence of cell clusters adherent on fibers'

surface **was observed**, in agreement with viability results (figure 2). This behavior could be due to the inefficacy of the seeding procedure, because of the inability of the polymeric meshes to retain a large number of cells. Nevertheless **a progressive increase of cells colonizing polymeric meshes was observed** for longer culture time points (7 and 14 days), as previously demonstrated from cell proliferation data. At day 14 cultured samples exhibited full cellular colonization of available fibers' surface by a wide continuous cell culture net.



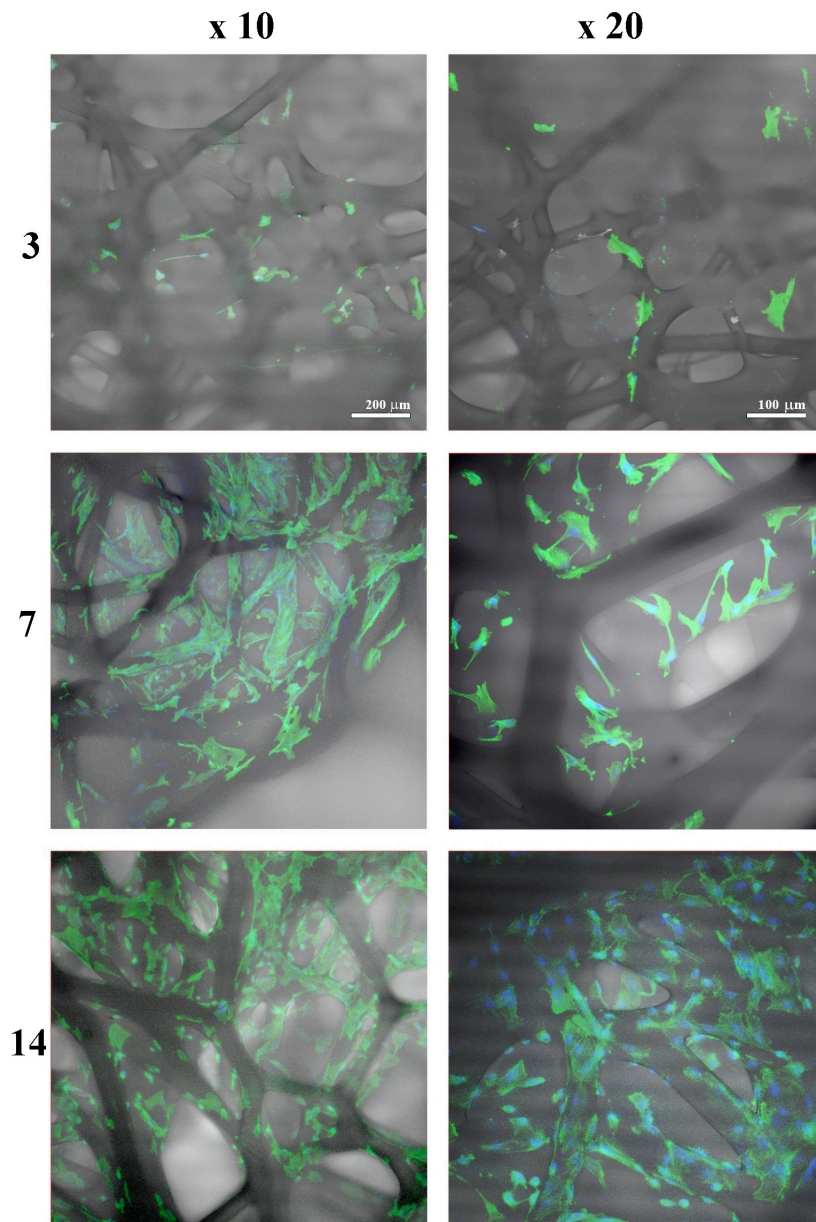


Figure 7. CLSM images (10X and 20X magnification) of balb/3T3 clone A31 cultured on \*PCL based scaffolds at different time of culture (3, 7 and 14 days).

Indirect immunofluorescence was used for the visualization of cytokeratins in order to discriminate HaCaT cell line from balb/3T3 clone A31 in the co-culture. Cytokeratins are typical proteins of intermediate filaments of cytoskeleton of epithelial cells ensuring mechanical stability and structural integrity of both the single

epithelial cells and, via cell-cell contacts, of that of the epithelial tissues<sup>53</sup>. Confocal **microscopy investigations** highlighted that cell lines, HaCaT and balb/3T3 clone A31, were able to colonize the fibers of the scaffolds. As shown in figure 8, the co-culture completely overlaid the scaffold, underlying the tendency to cover the polymeric fibers forming big colonies, resembling epithelial tissue, with areas with prevalence of fibroblasts. Mono-culture revealed more precisely 3D arrangement of the fibroblasts that prefer the fiber's intersection linking inter-fiber spaces and confirming their supporting role in the epithelial tissue's architecture<sup>54</sup>.

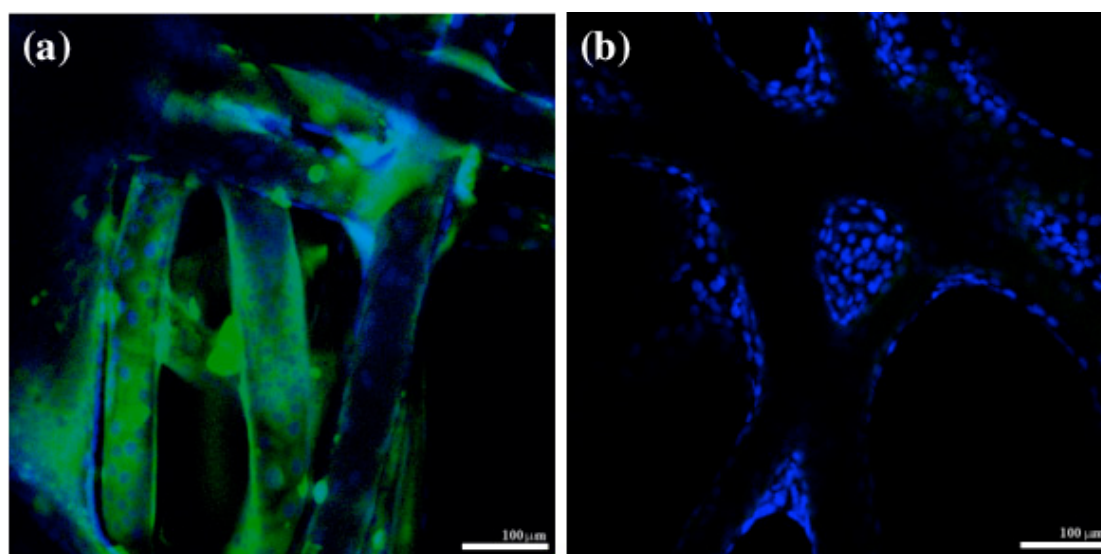


Figure 8. Cytokeratins visualization by immunofluorescence and DAPI staining of balb/3T3 Clone A31 and HaCaT grown in co-culture (a) and balb/3T3 Clone A31 in mono-culture (b) on \*PCL scaffolds (20X magnification).

Micrographs at higher magnification allowed the visualization of HaCaT morphology and cytoplasmic disposition of the keratins. HaCaT showed a typical polygonal shape with extremely reduced intracellular spaces (figure 9). Keratin, extended inside the

cytoplasm as a net, was able to cover the nucleus and connect the cell-cell junctions and desmosomes showing a pronounced fluorescence<sup>37, 53</sup>.

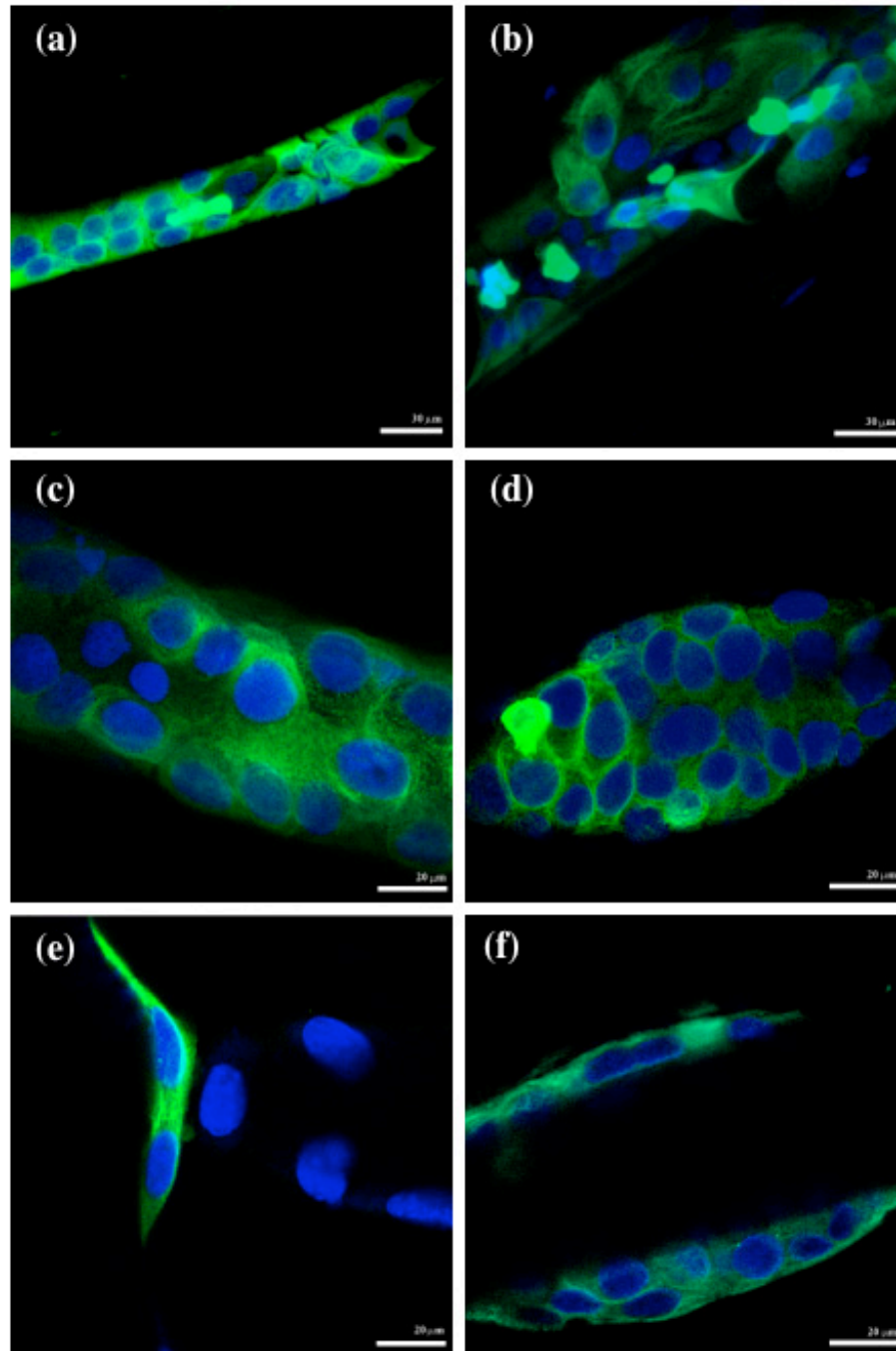


Figure 9. Cytokeratins visualization by immunofluorescence and DAPI staining of balb/3T3 Clone A31 and HaCaT grown in co-culture on \*PCL scaffolds at 60X (a,b) and 100X (c-f)

magnification.

## CONCLUSIONS

Microfibrinous \*PCL scaffolds were successfully prepared by using a melt-ES technique with a layer-by-layer approach. A preliminary screening was carried out in order to evaluate the suitability of the scaffolds as three-dimensional supports in the replacement of the natural ECM, by using mouse embryo fibroblast balb/3T3 clone A31 as cellular model. Scaffolds demonstrated to be able to support cell adhesion, proliferation and migration, preserving and increasing the ability of the cells to produce collagen, one of the main fibrillar component of the ECM <sup>55</sup>. Moreover, further studies to better investigate the suitability of the fibrous \*PCL scaffolds for wound dressing applications <sup>1</sup>, were carried out using co-cultures of mouse embryo fibroblasts and human keratinocytes. Scaffolds demonstrated their ability to support the growth of both cell lines. Moreover, cells were able to auto-organize them selves in a 3D structure, resembling the native architecture of epithelial tissues. Future studies will be carried out in order to confirm these *in vitro* results, by using *ex vivo* skin equivalent wound model.

## Acknowledgments

Authors are grateful to Dr. Aura Bonaretti for the recording of SEM images.

## References

1. Zhong SP, Zhang YZ, Lim CT. (2010). Tissue scaffolds for skin wound healing and dermal reconstruction. *Nanomedicine and Nanobiotechnology*. 2: 510-25.
2. Chong EJ, Phan TT, Lim IJ, Zhang YZ, Bay BH, Ramakrishna S, et al. (2007). Evaluation of electrospun PCL/gelatin nanofibrous scaffold for wound healing and layered dermal reconstitution. *Acta Biomaterialia*. 3: 321-30.
3. Clark R A F, Ghosh K, G TM. (2007). Tissue Engineering for Cutaneous Wounds. *J Invest Dermatol*. 127: 1018-29.
4. Sundaramurthi D, Vasanthan KS, Kuppan P, Krishnan UM, Sethuraman S. (2012). Electrospun nanostructured chitosan-poly(vinyl alcohol) scaffolds: a biomimetic extracellular matrix as dermal substitute. *Biomed Mater*. 7: 045005.
5. Falanga V, Faria K, Langer R, Vacanti J. (2007). Bioengineered skin constructs. *Principles of Tissue Engineering 3 rd ed Burlington: Academic Press*.
6. Detta N, Errico C, Dinucci D, Puppi D, Clarke D, Reilly G, et al. (2010). Novel electrospun polyurethane/gelatin composite meshes for vascular grafts. *Journal of Materials Science: Materials in Medicine*. 21: 1761-9.
7. Volpato F, Ramos SL, Motta A, Migliaresi C. (2011). Physical and in vitro biological evaluation of a PA 6/MWCNT electrospun composite for biomedical applications. *Journal of Bioactive and Compatible Polymers*. 26: 35-47.
8. Guarino V, Alvarez-Perez M, Cirillo V, Ambrosio L. (2011). hMSC interaction with PCL and PCL/gelatin platforms: A comparative study on films and electrospun membranes. *Journal of Bioactive and Compatible Polymers*. 26: 144-60.
9. Toncheva A, Spasova M, Paneva D, Manolova N, Rashkov I. (2011). Drug-loaded electrospun polylactide bundles. *Journal of Bioactive and Compatible Polymers*. 26: 161-72.
10. Bianco A, Bozzo BM, Del Gaudio C, Cacciotti I, Armentano I, Dottori M, et al. (2011). Poly (L-lactic acid)/calcium-deficient nanohydroxyapatite electrospun mats for bone marrow stem cell cultures. *Journal of Bioactive and Compatible Polymers*. 26: 225-41.
11. Hualin Z. (2011). Electrospun poly (lactic-co-glycolic acid)/multiwalled carbon nanotubes composite scaffolds for guided bone tissue regeneration. *Journal of Bioactive and Compatible Polymers*. 26: 347-62.
12. Kim SE, Heo D, Lee JB, Kim JR, Park SH, Jeon S, et al. (2009). Electrospun gelatin/polyurethane blended nanofibers for wound healing *Biomedical Materials*. 4: 044106.
13. Grafahrend D, Heffels K-H, Möller M, Klee D, Groll J. (2010). Electrospun, Biofunctionalized Fibers as Tailored in vitro Substrates for Keratinocyte Cell Culture. *Macromolecular Bioscience*. 10: 1022-7.
14. Bhardwaj N, Kundu SC. (2010). Electrospinning: A fascinating fiber fabrication technique. *Biotechnology Advances*. 28: 325-47.
15. Dalton P D, Calvet J, Mourran A, Klee D, Möller M. (2006). Melt electrospinning of poly(ethylene glycol-block- $\epsilon$ -caprolactone). *Biotechnology Journal*. 1: 998-1006.
16. Hutmacher DW, Dalton PD. (2011). Melt Electrospinning. *Chemistry – An Asian Journal*. 6: 44-56.
17. Pham QP, Sharma U, Mikos A. (2006). Electrospun poly( $\epsilon$ -caprolactone) microfiber and multilayer nanofiber/microfiber scaffolds: characterization of the scaffolds and measurement of cellular infiltration

*Biomacromolecules*. 7: 2796-805.

18. McKee MG, Unal S, Wilkes GL, Long TE. (2005). Branched polyesters: recent advances in synthesis and performance. *Prog Polym Sci*. 30: 507-39.

19. McKee M, Park T, Unal S, Yilgor I, Long T. (2005). Electrospinning of linear and highly branched segmented poly(urethane urea)s. *Polymer*. 46: 2011-5.

20. Xie W, Jiang N, Gan Z. (2008). Effects of Multi-Arm Structure on Crystallization and Biodegradation of Star-Shaped Poly( $\epsilon$ -caprolactone). *Macromolecular Bioscience*. 8: 775-84.

21. Hao Q, Li F, Li Q, Li Y, Jia L, Yang J, et al. (2005). Preparation and Crystallization Kinetics of New Structurally Well-Defined Star-Shaped Biodegradable Poly(l-lactide)s Initiated with Diverse Natural Sugar Alcohols. *Biomacromolecules*. 6: 2236-47.

22. Balakrishnan S, Krishnan M, Dubois P, Narayan R. (2004). Kinetic and thermodynamic considerations in the synthesis of a new three-arm poly( $\epsilon$ -caprolactone). *Polym Eng Sci*. 44: 1491-7.

23. Balakrishnan S, Krishnan M, Narayan R, Dubois P. (2006). Three-arm poly ( $\epsilon$ -caprolactone) by extrusion polymerization. *Polym Eng Sci*. 46: 235-40.

24. Puppi D, Detta N, Piras AM, Chiellini F, Clarke DA, Reilly GC, et al. (2010). Development of Electrospun Three-arm Star Poly( $\epsilon$ -caprolactone) Meshes for Tissue Engineering Applications. *Macromolecular Bioscience*. 10: 887-97.

25. Puppi D, Piras AM, Chiellini F, Chiellini E, Martins A, Leonor IB, et al. (2011). Optimized electro- and wet-spinning techniques for the production of polymeric fibrous scaffolds loaded with bisphosphonate and hydroxyapatite. *J Tissue Eng Regen Med*. 5: 253-63.

26. Puppi D, Dinucci D, Bartoli C, Mota C, Migone C, Dini F, et al. (2011). Development of 3D wet-spun polymeric scaffolds loaded with antimicrobial agents for bone engineering. *Journal of Bioactive and Compatible Polymers*. 26: 478-92.

27. Mota C, Puppi D, Dinucci D, Gazzarri M, Chiellini F. (2013). Additive manufacturing of star poly( $\epsilon$ -caprolactone) wet-spun scaffolds for bone tissue engineering applications. *Journal of Bioactive and Compatible Polymers*. Doi: In press.

28. Mota C, Puppi D, Gazzarri M, Bartolo P, Chiellini F. (2013). Melt-electrospinning writing of 3D star poly( $\epsilon$ -caprolactone) scaffolds. *Polymer International*. Doi: 10.1002/pi.4509.

29. Kirkpatrick CJ, Fuschs S, Unger RE. (2011). Coculture systems for vascularization *Learning from nature Advanced Drug Delivery Reviews* 63: 291-9.

30. Karchin A, Simonovsky FI, Ratner BD, Sanders JE. (2011). Melt electrospinning of biodegradable polyurethane scaffolds. *Acta Biomaterialia*. 7: 3277-84.

31. Park S, Lee S, Kim W. (2010). Fabrication of porous polycaprolactone/hydroxyapatite (PCL/HA) blend scaffolds using a 3D plotting system for bone tissue engineering. *Bioprocess and Biosystems Engineering*. 34: 505-13.

32. Stark HJ, Szabowski A, Fusenig NE, Szabowski NM. (2004). Organotypic cocultures as skin equivalents: A complex and sophisticated in vitro system. *Biol Proced Online*. 6: 55-60.

33. Puppi D, Mota C, Gazzarri M, Dinucci D, Gloria A, Myrzabekova M, et al. (2012). Additive manufacturing of wet-spun polymeric scaffolds for bone tissue engineering. *Biomedical Microdevices*. 14: 1115-27.

34. Kudelska-Mazur D, Malgorzata L-S, Mazur M, Komender J. (2005). Osteogenic cell contact with biomaterials influences phenotype expression. *Cell and Tissue Banking*. 6: 55-64.



35. Junqueira LCU, Bignolas G, Brentani RR. (1979). A Simple and Sensitive Method for the Quantitative Estimation of Collagen *Analytical Biochemistry*. 94: 96-9.
36. Soper DS. (2012). Analysis of Variance (ANOVA) Calculator - One-Way ANOVA from Summary Data (Online Software) <http://www.danielsoper.com/statcalc3>.
37. Schoop VM, Mirancea N, Fusenig NE. (1999). Epidermal Organization and Differentiation of HaCaT Keratinocytes in Organotypic Coculture with Human Dermal Fibroblasts. *The journal of investigative dermatology*. 112: 343-53.
38. Peschel G, Dahse H-M, Konrad A, Wieland GD, Mueller P-J, Martin DP, et al. (2008). Growth of keratinocytes on porous films of poly(3-hydroxybutyrate) and poly(4-hydroxybutyrate) blended with hyaluronic acid and chitosan. *Journal of Biomedical Materials Research Part A*. 85: 1072-81.
39. Maas-Szabowski N, Szabowski A, Stark H-J, Andrecht S, Kolbus A, Schorpp-Kistner M, et al. (2001). Organotypic Cocultures with Genetically Modified Mouse Fibroblasts as a Tool to Dissect Molecular Mechanisms Regulating Keratinocyte Growth and Differentiation. *J Investig Dermatol*. 116: 816-20.
40. Walter MNM, Wright KT, Fuller HR, MacNeil S, Johnson WEB. (2010). Mesenchymal stem cell-conditioned medium accelerates skin wound healing: An in vitro study of fibroblast and keratinocyte scratch assays. *Experimental Cell Research*. 316: 1271-81.
41. Rheinwald JG, Green H. (1975). Serial cultivation of strains of human epidermal keratinocytes: the formation keratinizing colonies from single cell is. *Cell*. 6: 331-43.
42. Owen SC, Shoichet MS. (2010). Design of three-dimensional biomimetic scaffolds. *Journal of Biomedical Materials Research Part A*. 94A: 1321-31.
43. Kempf M, Miyamura Y, Liu P-Y, Chen ACH, Nakamura H, Shimizu H, et al. (2011). A denatured collagen microfiber scaffold seeded with human fibroblasts and keratinocytes for skin grafting. *Biomaterials*. 32: 4782-92.
44. Auxefans C, Fradette J, Lequeux C, Germain L, Kinikoglu B, Bechetoille N, et al. (2009). Evolution of three dimensional skin equivalent models reconstructed *in vitro* by tissue engineering. *Eur J Dermatol*. 19: 107-13.
45. Chandrasekaran AR, Venugopal J, Sundarrajan S, Ramakrishna S. (2011). Fabrication of a nanofibrous scaffold with improved bioactivity for culture of human dermal fibroblasts for skin regeneration. *Biomed Mater*. 6 015001.
46. Lee DA, Assoku E, Doyle V. (1998). A specific quantitative assay for collagen synthesis by cells seeded in collagen-based biomaterials using sirius red F3B precipitation. *Journal of Materials Science: Materials in Medicine*. 9: 47-51.
47. Shariati SRP, Shokrgozar MA, Vossoughi M, Eslamifar A. (2009). In vitro co-culture of human skin keratinocytes and fibroblasts on biocompatible and biodegradable scaffold. *Iranian Biomedical Journal*. 13: 169-77.
48. Zhang B, Lalani R, Cheng F, Liu Q, Liu L. (2011). Dual-functional electrospun poly(2-hydroxyethyl methacrylate). *Journal of Biomedical Materials Research Part A*. 99A: 455-66.
49. Maas-Szabowski N, Stark HJ, Fusenig NE. (2000). Keratinocyte Growth Regulation in Defined Organotypic Cultures Through IL-1-Induced Keratinocyte Growth Factor Expression in Resting Fibroblasts. *The journal of investigative dermatology*. 114: 1075-84.
50. Sun T MS, Norton D, Haycock J W, Ryan A and MacNeil S

- (2005). Self-organization of skin cells in three-dimensional electrospun polystyrene scaffolds *Tissue Engineering*. 11: 1023-32.
51. Hutmacher DW, Schantz T, Zein I, Ng KW, Teoh SH, Tan KC. (2001). Mechanical properties and cell cultural response of polycaprolactone scaffolds designed and fabricated via fused deposition modeling. *Journal of Biomedical Materials Research*. 55: 203-16.
52. Kundu B, Kundu SC. (2012). Silk sericin/polyacrylamide in situ forming hydrogels for dermal reconstruction. *Biomaterials*. 33: 7456–67.
53. Moll R, Divo M, Langbein L. (2008). The human keratins: biology and pathology. *Histochemistry and Cell Biology*. 129: 705-33.
54. Sun T, Norton D, Ryan A, MacNeil S, Haycock J. (2007). Investigation of fibroblast and keratinocyte cell-scaffold interactions using a novel 3D cell culture system. *Journal of Materials Science: Materials in Medicine*. 18: 321-8.
55. Dutta RC, Dutta AK. (2010). Comprehension of ECM-Cell dynamics: A prerequisite for tissue regeneration. *Biotechnology Advances*. 28: 764-9.